Research & Reviews: Journal of Material Sciences
DOI: 10.4172/2321-6212.1000155

e-ISSN: 2321-6212
p-ISSN: 2347-2278

Direct Writing of Cu-based Micro-temperature Sensors onto Glass and Poly(dimethylsiloxane) Substrates Using Femtosecond Laser Reductive Patterning of CuO Nanoparticles

Mizoshiri M* and Hata S

Graduate School of Engineering, Nagoya University, Japan

Review Article

Received: 18/08/2016
Accepted: 04/10/2016
Published: 14/10/2016

***For Correspondence**

Mizoshiri M, Graduate School of Engineering, Nagoya University, Japan, Tel: +81-52-789-5031, Fax: +81-52-789-5032;

Email: mizoshiri@mech.nagoya-u.ac.jp

Keywords: Femtosecond laser, Reductive patterning, CuO nanoparticles, Direct-writing, Micro-temperature sensors

ABSTRACT

Micro-temperature sensors are fabricated directly onto glass and flexible Poly(dimethylsiloxane) (PDMS) substrates using femtosecond laser reductive patterning of CuO nanoparticles. Cu/Cu_2O composite micro-temperature sensors that consist of Cu_2O-rich sensing parts and Cu-rich electrodes are fabricated on glass substrates by controlling the reduction degree of CuO nanoparticles to Cu and Cu_2O. The sensor on the glass substrates has a large negative temperature coefficient of resistance. The conductive micropatterns fabricated on the PDMS substrates are Cu-rich only micropatterns. Cu-rich micro-temperature sensors are formed on the PDMS substrates, which exhibit a positive temperature coefficient of resistance. The temperature dependences of the sensors' resistance are consistent with those of Cu and Cu_2O. This selectively reductive method for patterning functional materials is useful for fabricating microdevices.

INTRODUCTION

Direct-writing technology has been widely studied for microfabrication processes. For example, metal and semiconductor conductive micropatterns, such as Ag, Au, and Cu micropatterns, have been fabricated by inkjet printing, laser sintering, and laser reductive sintering [1-13]. Inkjet fabrication consists of two steps: the micropatterning using metal Nanoparticle (NP) inks and annealing treatment for metallization [1-6]. On the other hand, laser sintering and reductive sintering allow micropatterning and metallization to be performed simultaneously in the so-called laser direct writing. Laser irradiation can be performed under ambient conditions. To date, low-resistivity Au, Ag, and Cu micropatterns have been fabricated by the laser sintering of their metal NP inks [7-10]. In laser reductive sintering, Cu and Ni micropatterns have been fabricated using laser-induced thermochemical reduction of copper oxide (CuO or Cu_2O) and NiO NPs, respectively [11-13]. Solution of metal oxide NPs, a reducing agent (reductant), and a dispersant were irradiated by focused laser light, resulting in the metal oxide NPs being reduced and sintered to form micropatterns. Ethylene Glycol (EG), 2-propanol, and Polyvinylpyrrolidone (PVP) were used as reductants and dispersants, respectively. In those laser irradiations, Continuous-Wave (CW) and nanosecond lasers were used for sintering. Compared to laser sintering of metal NPs, reductive sintering of metal oxide NPs leads to micropatterns with higher resistivity. However, the advantage of using metal oxide NPs with laser reductive sintering is that the metal oxide ones absorb the irradiated laser light more efficiently than the metal NP ones.

We have also developed femtosecond laser reductive patterning of CuO NPs [14-16]. In our process, Cu- and Cu_2O-rich micropatterns can be fabricated by controlling the reduction of CuO NPs [15,16]. Cu/Cu_2O composite micro-temperature sensors were fabricated on glass substrates using the selective micropatterning process. The Cu_2O-rich sensing part was effective because of its large negative temperature coefficient of resistance. The Cu-rich electrodes were thermally much stable and could be used in the micro-temperature sensors.

CuO NPs used in laser reductive sintering by CW and nanosecond lasers generally absorb the laser light energy effectively due to the band gap energy and their lower thermal conductivity. However, both reflectance and thermal conductivity of the re-

e-ISSN: 2321-6212
p-ISSN: 2347-2278

duced and sintered CuO NPs are expected to become higher during the laser irradiation because Cu is generated on the surface of the CuO NP solution films. Therefore, thermal reduction of CuO NPs becomes difficulty by reducing CuO NPs.

To date, the investigation of femtosecond laser ablation and heat effects of Cu has been reported by many research groups [17,18]. Cu bulks and thin films with higher reflectance and thermal conductivity were ablated by irradiating femtosecond laser pulses, which was enabled by shorter pulse duration than thermal diffusion time. This advantage has been also investigated by comparing femtosecond, picosecond, and nanosecond laser ablation of solid [19]. It is, therefore, femtosecond laser pulses are effective heat sources for metal fabrication. In femtosecond laser reductive sintering, CuO NP solution films were reduced and sintered efficiently in the film thickness direction by inhibiting thermal diffusion and heat losses induced by higher Cu thermal conductivity, even though Cu thin films were formed on the CuO NP solution films during their reduction and sintering.

In this paper, we review the fabrication of Cu-based micro-temperature sensors on the glass and flexible Poly(dimethylsiloxane) (PDMS) substrates using femtosecond laser reductive patterning [15,16]. First, we investigate the patterning properties on both the glass and PDMS substrates. Then, we fabricate Cu-based micro-temperature sensors and evaluate their properties.

EXPERIMENTAL

Fabrication Process of Micro-temperature sensors Using Femtosecond Laser Reductive Patterning

Schematic illustrations of the micro-temperature sensors developed using femtosecond laser reductive patterning of CuO NPs are shown in **Figure 1**. First, a solution of CuO NPs, a reductant agent, and a dispersant is spin-coated onto the substrates. Then, the electrodes and the sensing part are formed by femtosecond laser-induced thermochemical reduction of the CuO NPs. The Cu- and Cu_2O-rich micropatterns are fabricated by controlling the femtosecond laser irradiation conditions. Finally, non-irradiated CuO NPs are removed by rinsing the substrates in EG and ethanol.

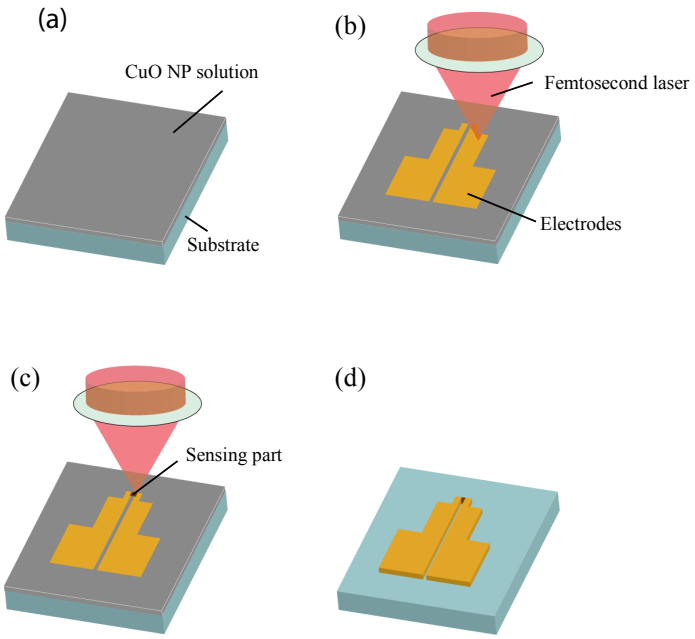

Figure 1: Fabrication process of Cu/Cu_2O composite micro-temperature sensors using femtosecond laser reductive patterning of CuO NPs. (a) coating of CuO NP solution film on the substrates, femtosecond laser reductive patterning for (b) the electrodes and (c) the temperature sensing part, and (d) removal of non-irradiated CuO NPs.

The femtosecond laser pulses are focused onto the surface of the CuO NP solution film using an objective lens with a numerical aperture of 0.80. The pulse duration, wavelength, and repetition frequency of the femtosecond fiber laser (Toptica, FemtoFiber, Pro NIR) are 120 fs, 780 nm, and 80 MHz, respectively. The maximal pulse energy with which the samples are irradiated is 0.62 nJ. Laser writing is carried out by scanning the substrate using XYZ mechanical stages. The scan speed is varied from 0.5 to 20 mm/s.

Material Preparation

CuO NPs are prepared using the ultrasonic waves to mix CuO NPs (particle size <50 nm; Sigma Aldrich), EG (Sigma Aldrich) as a reductant, and PVP (M_w ~10,000; Sigma Aldrich) as a dispersant. The concentrations of CuO NPs, EG, and PVP are 60 wt%, 27 wt%, and 13 wt%, respectively. First, EG and PVP are mixed ultrasonically using an ultrasonic homogenizer (UH-50; MST Co., Ltd.). Then, the CuO NPs are additionally mixed ultrasonically with the EG/PVP solution.

The CuO NP solutions are spin-coated onto the substrates at 7000 rpm. Both the glass and flexible PDMS substrates are

e-ISSN: 2321-6212
p-ISSN: 2347-2278

used, each with a thickness of 1 mm. PDMS substrates are prepared using a mixture of PDMS Sylgard Silicone Elasomer 184 and Sylgard Curing Agent 184 (Dow Corning Co.). The concentration ratio of the elastomer and curing agent is 10:1. The PDMS is cured by baking it at 70°C for 30 min.

Evaluation of Micropatterns and Micro-temperature Sensors

The crystalline of the micropatterns are examined using an X-ray micro-diffractometer (RINT RAPID-S; Rigaku Co.) equipped with a Cu-Kα radiation source. The micropatterns are irradiated on an X-ray beam collimated to 0.3 mm diameter at an incident angle of 20°. The electrical resistivity of the fabricated micropatterns is examined using a four-terminal system (Loresta GP; Mitsubishi Chemical Analytech).

The micro-temperature sensors are evaluated in relation to the temperature dependence of their resistance. This is measured using an electronic multimeter under various temperatures that are controlled using a hot plate in air. The metastable Cu_2O-rich micropatterns in the micro-temperature sensors are overcoated with 100 nm-thick SiO_2 thin films using the radio-frequency magnetron sputtering method to prevent reoxidation during the evaluation.

RESULTS AND DISCUSSIONS

Line Widths on Glass or PDMS Substrates

The width of the lines written by femtosecond laser reductive patterning on the glass and PDMS substrates are shown in **Figure 2**. The pulse energy is 0.54 nJ. On both substrates, the line width is decreased by increasing the scan speed on the both substrates. The lines on PDMS are wider than those on glass for the same scan speed. When the femtosecond laser pulses are irradiated on CuO NP solution films, the laser light is absorbed and converted to thermal energy. The thermal energy is partially used to reduce and sinter CuO NPs. However, the remained thermal energy is accumulated and diffused into CuO NP solution films. The accumulated thermal energy is also diffused to the substrates. When the thermal conductivity is lower, the accumulated thermal energy is easily diffused into CuO NP solution films in the film planar direction than into the substrates. The thermal conductivity of PDMS is known to be higher than that of glass [20]. As a result, the lines on PDMS substrates are wider than those on glass substrates.

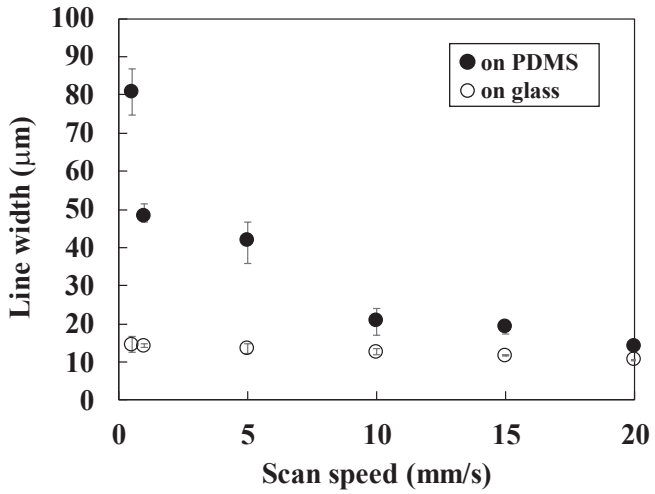

Figure 2. Dependence of scan speed on the width of lines formed on the PDMS and the glass substrates.

Crystalline Structure and Resistance of the Micropatterns (glass)

The micropatterns used for X-ray diffraction (XRD) analysis are prepared by raster scanning the glass substrates with pitches of 5, 10, and 15 μm. The XRD spectra of the micropatterns at a raster scan pitch of 5 μm are shown in **Figure 3**. The scan speeds are 1, 5, 10, 15, and 20 mm/s, and the pulse energy is 0.54 nJ. All the fabricated micropatterns contain Cu, Cu_2O, and CuO. There is a significant difference between the XRD spectra for scan speeds >5 mm/s and those for 1 mm/s. Large intensity peaks corresponding to Cu are observed for scan speeds >5 mm/s, although weaker-intensity peaks corresponding to Cu are observed for 1 mm/s. These results indicate that Cu-rich and Cu_2O-rich micropatterns are selectively fabricated by controlling the laser irradiation conditions.

We compare the XRD diffraction peaks of Cu, Cu_2O, and CuO to evaluate the reduction degree of the micropatterns. The value of $I_{Cu2O(111)}/I_{CuO(111)}$, which is calculated as the ratio of the peak intensity of $Cu_2O(111)$ to that of CuO(111), is used to evaluate Cu_2O generation. The value of $I_{Cu(111)}/I_{Cu2O(111)}$, which is calculated as the ratio of the peak intensity of Cu(111) to that of $Cu_2O(111)$, is used to evaluate Cu generation against Cu_2O. **Figure 4a-4c** show the degree of Cu_2O generation against CuO in micropatterns that are fabricated at scan pitches of 5, 10, and 15 μm, respectively. Cu_2O generation increases with decreasing scan pitch at constant scan speed and pulse energy. The maximum $I_{Cu2O(111)}/I_{CuO(111)}$ value occurs for a scan speed and pitch of 1 mm/s and 5

e-ISSN: 2321-6212
p-ISSN: 2347-2278

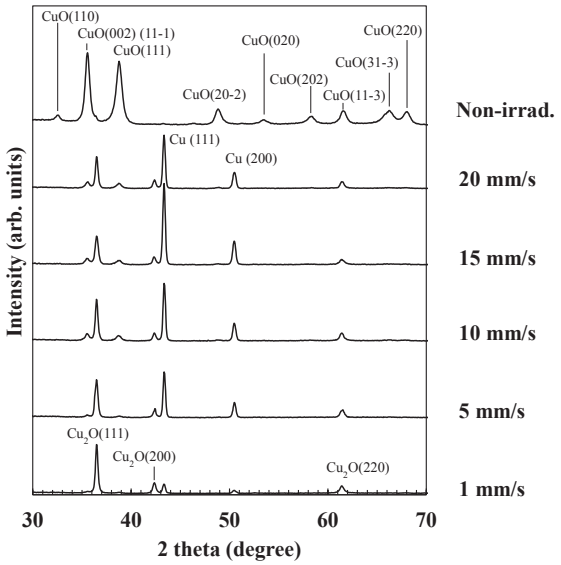

Figure 3. XRD spectra of the micropatterns (raster scan pitch: 5 μm) fabricated on glass substrates with various scan speeds at a pulse energy of 0.54 nJ [16].

μm, respectively. To date, Cu_2O-rich micropatterns have exhibited a large negative Temperature Coefficient of Resistance (TCR) [15]. The Cu_2O-rich sensing part of the micro-temperature sensors is therefore formed under this condition.

Figure 4d-4f show the degree of Cu against Cu_2O at scan pitches of 5, 10, and 15 μm, respectively. The maximum value of $I_{Cu(111)}/I_{Cu2O(111)}$ occurs for a scan speed of 10 mm/s and the scan pitch of 15 μm. In contrast, the values of $I_{Cu2O(111)}/I_{Cu(111)}$ at a pitch of 15 μm are as low as 0.1–0.4, as shown in **Figure 4f**. This relatively low Cu_2O generation is used to form low-resistance Cu-rich micropatterns at a scan speed of 15 mm/s and a pulse energy of 0.45 nJ, as shown in **Figure 4d and 4e**. The Cu-rich electrodes of the micro-temperature sensors can also be fabricated using this laser irradiation condition.

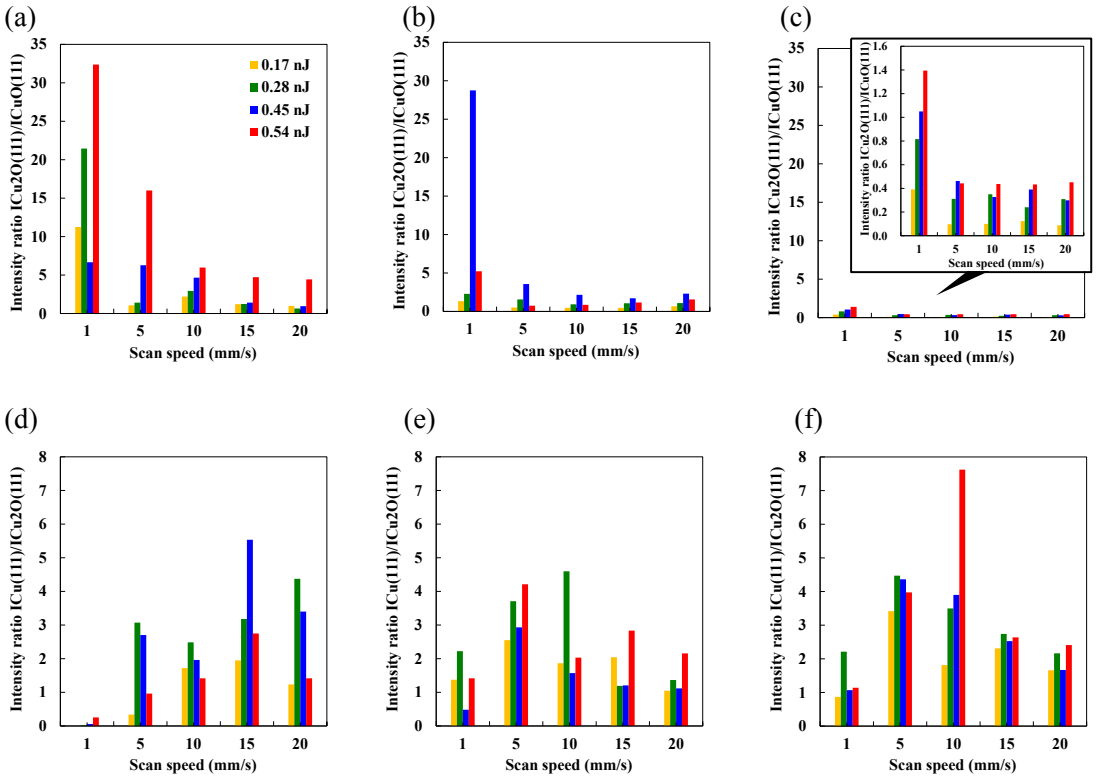

Figure 4. Intensity ratio of $I_{Cu2O(111)}/I_{CuO(111)}$ at a scan pitch of (a) 5 μm, (b) 10 μm, and (c) 15 μm. Intensity ratio of $I_{Cu(111)}/I_{Cu2O(111)}$ at a scan pitch of (d) 5 μm, (e) 10 μm, and (f) 15 μm. All micropatterns were formed on glass substrates [16].

Cu_2O generation increases with the total laser energy. However, the maximum Cu generation occurs for a relatively higher laser scan speed of 15 mm/s, i.e., not by increasing the total laser energy. This suggests that Cu_2O is generated by reoxidation of the reduced Cu that is at a scan speed of 1 mm/s.

e-ISSN: 2321-6212
p-ISSN: 2347-2278

The electrical resistivities of the Cu_2O- and Cu-rich micropatterns are ~10 Ωm and ~9 μΩm, respectively, the micropatterns are assumed to be 8 μm thick.

Crystalline Structure and Resistance of Micropatterns (PDMS)

Figure 5 shows XRD spectra of the micropatterns on the PDMS substrates. The pulse energy is 0.54 nJ, and the scan speeds are 0.5, 1.5, 10, 15, and 20 mm/s, respectively. In contrast to the micropatterns on the glass substrates, micropatterns on the PDMS substrates for a pulse energy of 0.54 nJ and a scan speed of 1 mm/s contain more Cu than Cu_2O. By increasing the total irradiation energy by reducing the scan speed, Cu_2O-rich micropatterns are obtained by reoxidizing the reduced Cu at a scan speed of 0.5 mm/s. These results indicate that the micropatterning on the PDMS does not easily reoxidize the reduced Cu. There are two possible reasons for this. One is that lines on the PDMS substrates are wider than those on the glass ones, as shown in **Figure 2**. Therefore, the volume of the reduced Cu on PDMS substrates is larger than that on glass substrates. When the volume of Cu with lower thermal conductivity increased, it prevented the micropatterns from reoxidizing during laser raster scanning. The second possible reason is that the PDMS substrates themselves act as the reductant when both the CuO NP solution and its underlying PDMS substrate are heated by femtosecond laser irradiation. PDMS is a more unstable material than glass. In addition, it includes carbon and hydrogen atoms which possibly reduce copper oxides such as Cu_2O and CuO. As a result, reoxidation might be prevented in the case of the micropatterning on PDMS substrates.

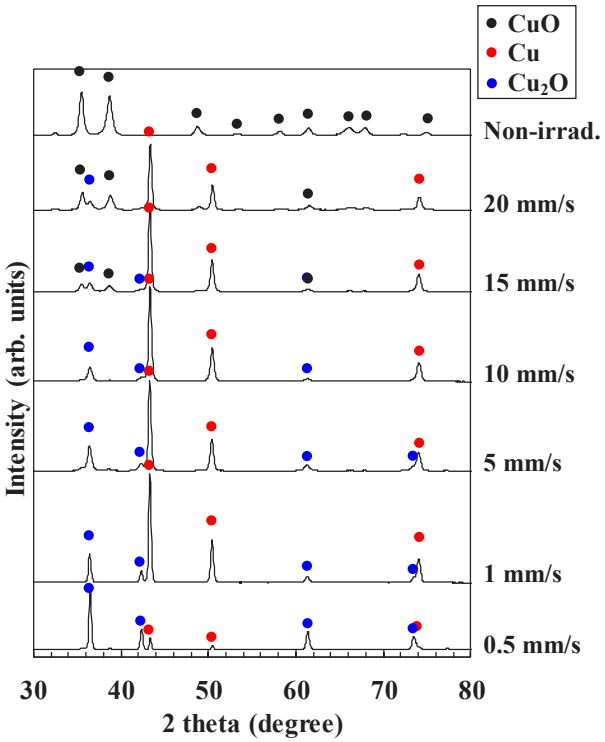

Figure 5. XRD spectra of the micropatterns (raster scan pitch: 5 μm) fabricated on PDMS with various scan speeds at a pulse energy of 0.54 nJ.

To evaluate the Cu generation against Cu_2O, the XRD peak intensity ratio, $I_{Cu(111)}/I_{Cu2O(111)}$ is calculated in the same way as that for micropatterns on glass substrates. **Figure 6** shows the dependence of scan speed on the intensity ratio $I_{Cu(111)}/I_{Cu2O(111)}$. The pulse energies are 0.44, 0.54, and 0.62 nJ. The maximum Cu generation against Cu_2O is obtained at a scan speed of 15 mm/s and a pulse energy of 0.54 nJ. The micropatterns fabricated at a pulse energy of 0.54 nJ give the largest Cu generation against Cu_2O. This result suggests that microstructures fabricated at a pulse energy of 0.62 nJ are reoxidized by excessive total laser energy, resulting in Cu_2O being generated by reoxidizing of the reduced Cu micropatterns. However, the micropatterns fabricated at a pulse energy of 0.44 nJ contain the lowest Cu ratio against Cu_2O. We consider that lower total laser energy induces the lower Cu generation and higher Cu_2O generation.

Figure 7 shows the relationship between the resistivity of the micropatterns at a pulse energy of 0.54 nJ and the scan speed. The micropatterns are 20-mm long and 0.5-mm wide. The film thickness is ~8 μm. When the scan speed is 0.5 mm/s (i.e., the only Cu_2O-rich generation condition), the micropatterns are not electrically conductive. An optical microscope image of the micropatterns is shown in the inset of **Figure 7**. Numerous microcracks can be seen on the surface of the micropatterns, indicating that they are not electrical conductive. These microcracks are possibly formed by expansion and shrinkage of the PDMS substrates caused by excessive heating and cooling. The lowest resistivity of the micropatterns is obtained at a scan speed of 15 mm/s. By comparing the Cu generation against the Cu_2O in the micropatterns, as shown in **Figure 6**, we see that those with the maximum Cu have the highest electrical conductivity under these laser irradiation conditions. Thus, the Cu generation ratio in the microstructures is consistent with resistivity.

e-ISSN: 2321-6212
p-ISSN: 2347-2278

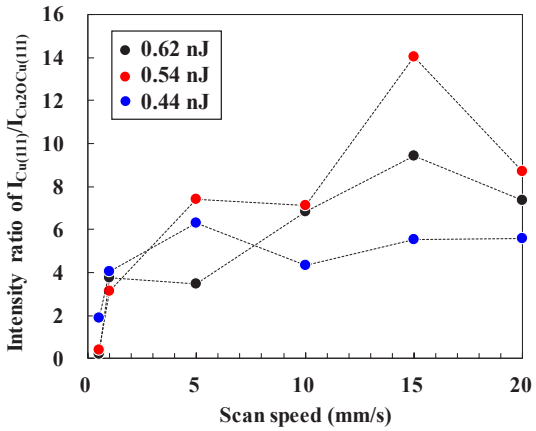

Figure 6. Intensity ratio of $I_{Cu2O(111)}/I_{CuO(111)}$ at a scan pitch of (a) 5 μm, (b) 10 μm, and (c) 15 μm. Intensity ratio of $I_{Cu(111)}/I_{Cu2O(111)}$ at a scan pitch of (d) 5 μm, (e) 10 μm, and (f) 15 μm. All micropatterns were formed on PDMS substrates.

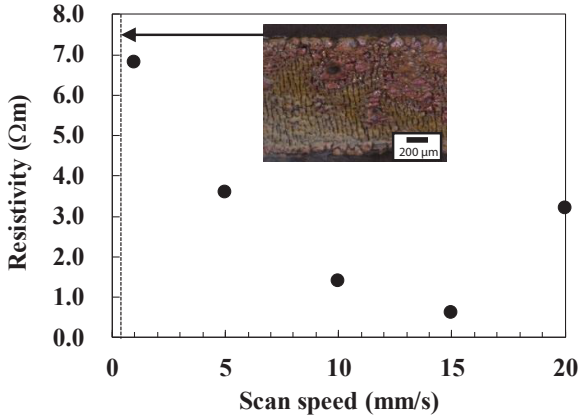

Figure 7: Relationship between the resistivity of the microstructures on PDMS substrates and the scan speed. Inset: optical microscope image at a scan speed of 0.5 mm/s.

Fabrication of Cu-based Micro-temperature Sensors

Figure 8 shows the design of the Cu-based micro-temperature sensors fabricated using femtosecond laser reductive patterning of CuO NPs. The sensing part on the glass and PDMS substrates is Cu_2O-rich and Cu-rich micropatterns, respectively.

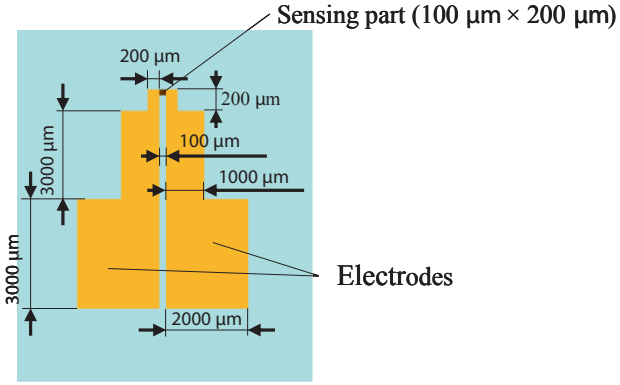

Figure 8: Schematic of the design of a micro-temperature sensor.

Cu/Cu_2O composite micro-temperature sensors are fabricated on the glass substrate. The Cu_2O-rich sensing part and the Cu-rich electrodes are selectively fabricated by controlling the laser irradiation conditions. The Cu_2O- and the Cu-rich micropatterns are written at scan speeds and pulse energies of 1 mm/s and 0.54 nJ, and 15 mm/s and 0.45 nJ, respectively. **Figure 9a** shows an optical microscope image of the fabricated Cu_2O-rich sensing part and Cu-rich electrodes. After the non-irradiated CuO NPs are removed and SiO_2 thin film is overcoated onto the Cu_2O-rich sensing part, the resistance of the micro-temperature sensors is measured under various temperatures on a hot plate. The temperature dependence of the resistance of the micro-temperature sensors is shown in **Figure 9b.** The resistance decreases with increase in temperature, and is 25.73 MΩ at 30°C. This value is

e-ISSN: 2321-6212
p-ISSN: 2347-2278

~10 MΩ larger than the one estimated using the electrical resistivities of Cu_2O- and Cu-rich micropatterns, namely ~10 Ωm and ~9 μΩm, respectively. The TCR of the micro-temperature sensors is -5.5×10^{-3}/°C. This negative value of TCR is consistent with that of semiconductor Cu_2O.

A Cu-rich micro-temperature sensor is fabricated on a PDMS substrate. **Figure 10a and 10b** show an optical microscope image and the temperature dependence of resistance, respectively. The fact that the TCR is a positive is consistent with the crystalline structures of the Cu-rich micropatterns.

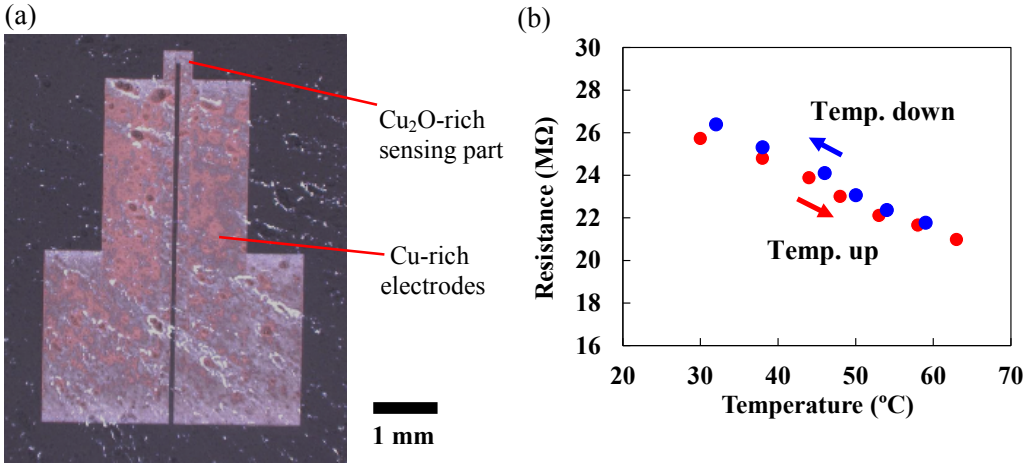

Figure 9. (a) Optical microscope image and (b) temperature dependence of resistance of a Cu/Cu_2O composite micro-temperature sensor on glass substrate [16].

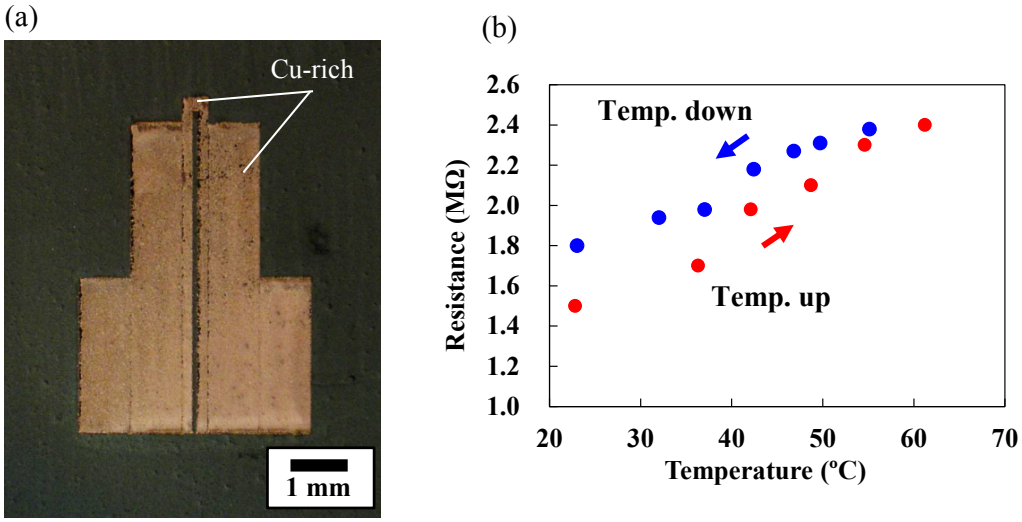

Figure 10: (a) Optical microscope image and (b) temperature dependence of resistance of a Cu-rich micro-temperature sensor on a PDMS substrate.

By comparing the Cu_2O- and Cu-rich micro-temperature sensors, we found that the Cu_2O-rich one is the more sensitive of the two. The absolute TCR value of metal Cu is larger than that of semiconductor Cu_2O. The resistance properties of the micro-temperature sensors are consistent with their bulk material properties. This femtosecond laser reductive patterning is an advantageous for fabricating microdevices that consist of functional composite materials.

CONCLUSIONS

We fabricated two-types of micro-temperature sensors using femtosecond laser reductive patterning of CuO NPs. The Cu/Cu_2O composite micro-temperature sensors that contained a Cu_2O-rich sensing part and Cu-rich electrodes were fabricated by selective reduction of CuO NPs controlled by laser irradiation. Cu-rich micro-temperature sensors were fabricated on flexible PDMS substrates. This femtosecond laser reductive patterning is advantageous for fabricating microdevices.

ACKNOWLEDGMENTS

This study was partially supported by the Nanotechnology Platform Program (Micro-Nano Fabrication) of the Ministry of Education, Culture, Sports, Science and Technology, Japan (MEXT), by the Cross-ministerial Strategic Innovation Promotion Program (SIP) of the New Energy and Industrial Technology Development Organization (NEDO), and by the Amada Foundation (AF-

e-ISSN: 2321-6212
p-ISSN: 2347-2278

2014206).

References

1. Perelaer J, et al. Ink-jet printing and microwave sintering of conductive silver tracks. Adv Mater 2006:18:2101-2104.
2. Park BK, et al. Direct writing of copper conductive patterns by ink-jet printing. Thin Solid Films 2007:515:7706-7711.
3. Jeong S, et al. Controlling the thickness of the surface oxide layer on Cu nanoparticles for the fabrication of conductive structures by ink-jet printing. Adv Func Mater 2008:18:679-686.
4. Woo K, et al. Ink-jet printing of Cu-Ag based highly conductive tracks on a transparent substrate. Langmuir 2009:25:429-433.
5. Goo Y-S, et al. Ink-jet printing of Cu conductive ink on flexible substrate modified by oxygen plasma treatment. Surf Coat Technol 2010:205:S369-S372.
6. Cui W, et al. Gold nanoparticle ink suitable for electric-conductive pattern fabrication using in ink-jet printing technology. Colloids and Surfaces A: Physicochem Eng Aspects 2010:358:35-41.
7. Aminuzzaman M, et al. Direct writing of conductive silver micropatterns on flexible polyimide film by laser-induced pyrolysis of silver nanoparticle-dispersed film. J Nanopart Res 2010:12:931-938.
8. Michael Z, et al. Laser sintering of copper nanoparticles. J Phys D: Appl Phys 2013:47:025501.
9. Gang Q, et al. Conductive network structure formed by laser sintering of silver nanoparticles. J Nanopart Res 2014:16:2684.
10. Gang Q, et al. Copper film prepared from copper fine particle paste by laser sintering at room temperature: Influences of sintering atmosphere on the morphology and resistivity. Jpn J Appl Phys 2014:53:096501.
11. Kang B, et al. One-step fabrication of copper electrode by laser-induced direct local reduction and agglomeration of copper oxide nanoparticle, J Phys Chem C 2011:115:23664-23670.
12. Lee D, et al. Vacuum-free, maskless patterning of Ni electrodes by laser reductive sintering of NiO nanoparticle ink and its application to transparent conductors. ACS Nano 2014:8:9807-9814.
13. Paeng D, et al. Laser-induced reductive sintering of nickel oxide nanoparticles under ambient conditions. J Phys Chem C 2015:119:6363-6372.
14. Arakane S, et al. Direct patterning of Cu microstructures using femtosecond laser-induced CuO nanoparticle reduction. Jpn J Appl Phys 2015:54:06FP07.
15. Mizoshiri M, et al. Direct writing of Cu-based micro-temperature detectors using femtosecond laser reduction of CuO nanoparticles. Appl Phys Express 2016:9:036701.
16. Mizoshiri M, et al. Direct fabrication of Cu/Cu2O composite micro-temperature sensor using femtosecond laser reduction patterning. Jpn J Appl Phys 2016:55:06GP05.
17. Hirayama Y, et al. Heat effects of metals ablated with femtosecond laser pulses. Appl Sur Sci 2002:197-198:741-745.
18. Hirayama Y, et al. Heat-affected zone and ablation rate of copper ablated with femtosecond laser. J Appl Phys 2005:97:064903.
19. Chichkov BN, et al. Femtosecond, picosecond and nanosecond laser ablation of solids. Appl Phys A 1996:63:109-115.
20. Yamamoto T, et al. PDMS-glass hybrid microreactor array with embedded temperature control device. Application to cell-free protein synthesis. Lab Chip 2002:2:197-202.